Department of Energy Final Scientific/Technical Report

Award Number: DE-DE-FC26-06NT42932
Title: An Integrated Solid-State LED Luminaire for General Lighting
Principal Investigator: Kevin Dowling, Color Kinetics
Team Members

Color Kinetics
Kevin Dowling, Fritz Morgan, Ihor Lys, Mike Datta,
Cree Inc, Santa Barbara Technology Center
Bernd Keller, Thomas Yuan, Monica

Executive Summary

A strong systems approach to designing and building practical LED-based replacement lamps is lacking. The general method of taking high-performance LEDs and marrying them to standard printed circuit boards, drivers and a heat sink has fallen short of the promise of LED lighting. In this program, a top-down assessment of requirements and a bottom-up reinvention of LED sources, electronics, optics and mechanics have resulted in the highest performance lamp possible.

The team, comprised of Color Kinetics, the leaders in LED lighting and Cree, the leaders in LED devices took an approach to reinvent the package, the driver and the overall form and aesthetic of a replacement source. The challenge was to create a new benchmark in LED lighting - the resultant lamp, a PAR38 equivalent, met the light output, color, color quality and efficacy marks set out in the program as well as being dimmable, which is important for market acceptance.

The approach combined the use of multiple source die, a chip-on-board approach, a very efficient driver topology, the use of both direct emission and phosphor conversion, and a unique faceted optic to avoid the losses, artifacts and hotspots of lensed approaches. The integral heat sink provided a mechanical base and airflow using a chimney-effect for use in a wide variety of locations and orientations.

These research results led to a much better understanding of the system effects of component level technologies. It was clear that best-of-breed sub-system results do not necessarily result in the best end result for the complete system.

In doing this work, we did not neglect the practical aspects of these systems. These were not rarified results and commercially impractical but lent themselves to eventual commercial products in the marketplace. The end result - a high performance replacement lamp - will save significant energy while providing a high-quality light source.

DISCLAIMER

Introduction

As shown in the figure on the right, lighting specifiers do not necessarily think of lighting in terms of lamps and fixtures. The primary goal is good quality lighting and the lamps and fixtures from myriad manufacturers are but tools to create a solution. In this picture, the specifier's desire, given practical constraints, is to light the merchandise in a retail setting. The designer thinks about shadow, contrast, depth and ambiance in making their decision about lighting configurations and sources.

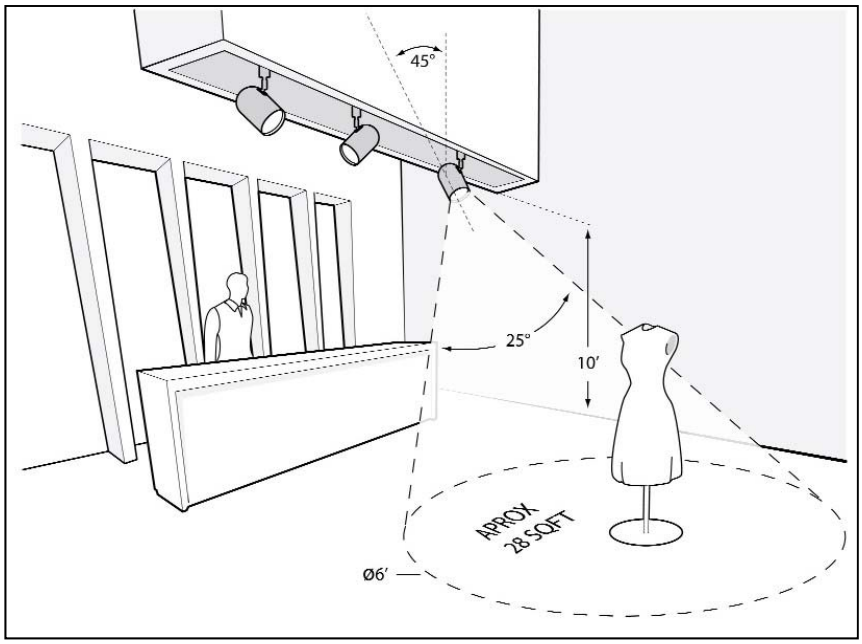

Figure 1. Perspective of lighting as a result the rather.

In the LED industry, the mindset has been otherwise and the solution has generally been to take the highest performance light-emitting diodes, LEDs, and populate a lamp-like form-factor to provide lighting solutions that designers would then use. Unfortunately, this approach, while easy, is short-sighted and reduces the quality of the overall light. While the numbers may show adequate performance, the real-world nature of these systems is often below par due to poor color quality, poor output distribution, sub-standard light output and more.

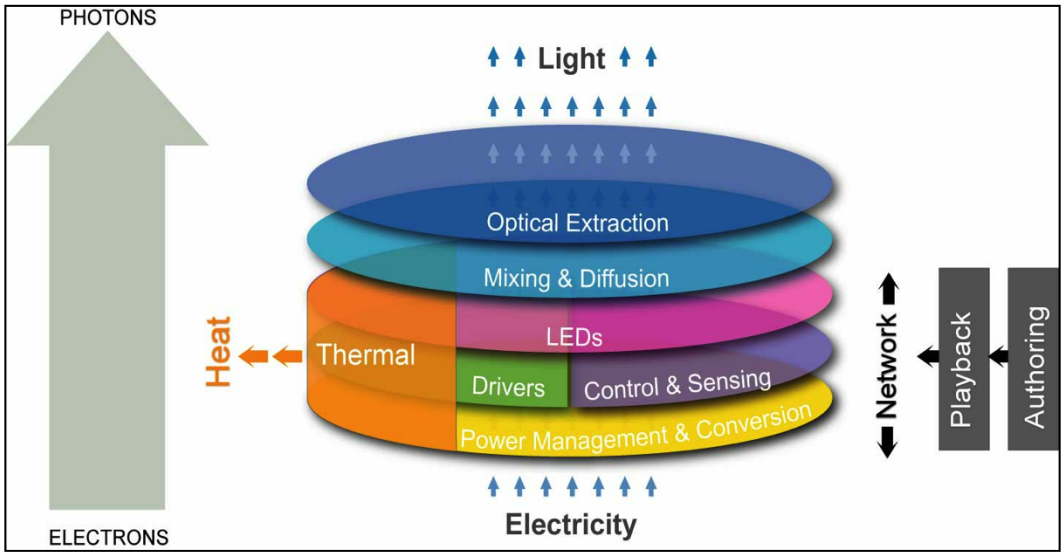

Figure 2. An LED system is comprised of much more than an LED device. All sub-systems, in aggregate, constrain and define the system performance.

In this project we envisioned a new approach to the system design and the construction of an LED-based light source. We deconstructed the LED source and rethought the integrated driver,

optics, thermal management, and mechanics of the system. It required the reinvention of the LED package and the electronics to drive them. The end result is a very high quality lighting source.

Lamp Form Factor

Parabolic Reflector lamps are used for spot lighting applications. It is no accident that PAR lamps have particular characteristics and are widely used for these types of lighting applications. So too are metallized reflectors, MR lamps and AR-111s. In general, as shown in Figure 3, for a given ceiling height and lighting angle, the beam geometry is approximately 25-30 degrees with a uniform output to appropriately light merchandise and provide an appropriately sized circle of light at merchandise height. But PARs are widely used in flood and spot applications as well. Unlike the traditional Edison-style A19 lamp, the PAR lamp light output is in a single direction. This makes the lamp less efficient overall, but it is very good at throwing lighting in a particular direction.

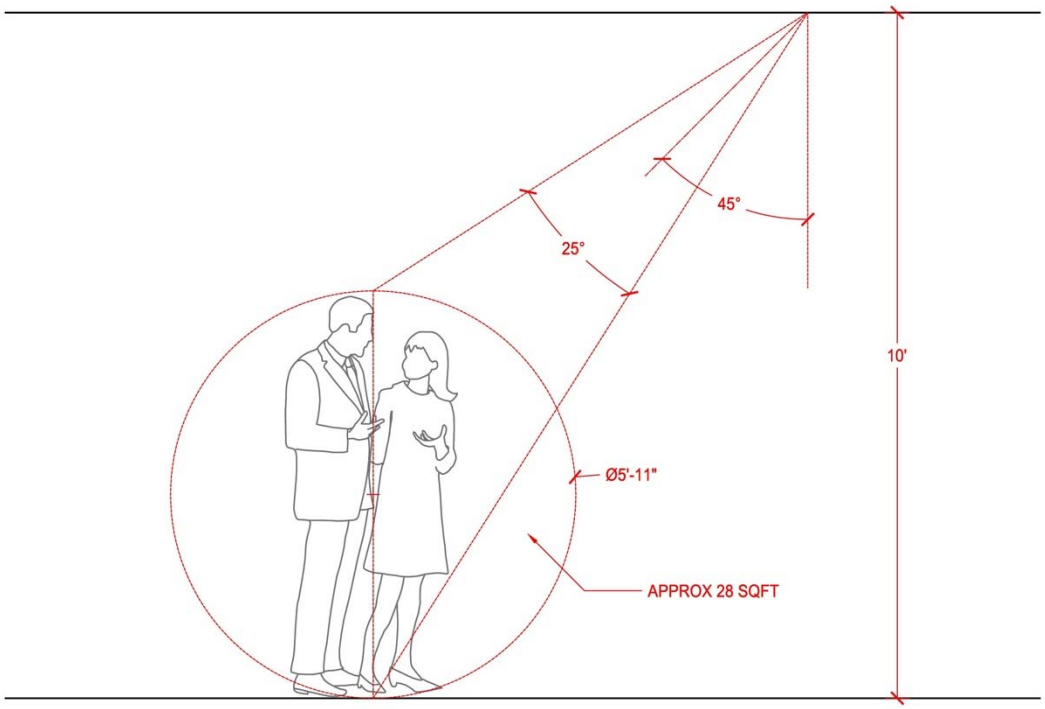

Figure 3. Beam geometry in a typical application.

The PAR can be ideal for LED lighting because their design, directs light well. An LED die, the semiconductor chip within the package, is actually omnidirectional, but the practical issues of containing the die and providing electrical current to the die as well as heat sinking of the die, usually constrain the device to emit in one hemisphere only.

While integration is a key aspect to our program and project results, in this report we will focus on the individual tasks associated with optical modeling, thermal considerations and a key component of direct emission and phosphor conversion LEDs.

Light Source

One of the first joint tasks was to define a light source comprised of LED devices. The traditional approach of making large die and driving them with high currents in the range of 0.5 to 1.0A did result in more light but also high losses. Similar to a big car engine that can deliver more power but lower mileage, this approach had diminishing returns in LED lighting.
We developed an approach using large numbers of smaller die which resulted in higher efficiencies but also complicated the optical properties of the system. Thus, a clear evaluation of the optical properties was required.

Strength in Numbers: LED configuration
The typical approach for high output systems is to use high power LEDs. But we felt that viable and efficient alternatives existed using a greater number of smaller chips. We evaluated this approach and saw a number of benefits from a larger number of smaller die. These included:

Optical: The denser constellation of points produce a more uniform light output improving color mixing, glare and luminance (i.e. mitigating the 'Lite-Brite®' effect).
Electrical: Lower currents associated with a larger number of serialized die mean that lower current, and thus lower cost, devices can be used to drive the LEDs.
Thermal: The power density of a larger number of smaller die is much lower and overall thermal qualities improve markedly.
Packaging: The die approach or even a small package approach should be lower cost than a small number of large high-power packages.
Cost: We don't see any significant cost issues. Small die are less expensive than the equivalent-area large die. Lifetime ownership costs should also improve.
Efficiency: The combination of the electrical, thermal and optical benefits can yield greater efficiencies in the integrated system.
Yield: A downside is that, for a given failure rate, a larger number of parts will inevitably lead more placement or wiring failures. However, we developed innovative designs providing redundancy and evaluated, but did not implement, means to potentially bypass improperly packaged parts.

Spectral Properties
Since LEDs emit light of only one narrow-band color, then white light can be created through just a few methods, including combinations of colors such as red, green, and blue, or the use of wavelength shifting materials such as phosphors. White LEDs primarily use phosphor conversion to shift blue wavelengths into the green and red regions. The result due to this shift is white light. However, the quality of white light created in this way can vary significantly and can often result in poor quality light. The quality of a light source is defined by its color quality, usually measured by the color rendering index, CRI, as well as its color temperature, CT, or if away from the black-body curve, its correlated color temperature, CCT. The shift of blue frequencies up into the red region is quite inefficient and results from Stokes Shift losses, which are greater with the 'distance' of wavelength shift.

To create a good, efficient and high quality light we evaluated a combination of direct emission LEDs in the red region combined with white LEDS. This provided a clean way of creating a good light but also meant that the optical subsystem would not be combining a number of point sources of different spectral power distribution or SPD.

A significant effort in optical modeling was required to evaluate whether or not this was a viable approach.

Optical Modeling

We performed optical modeling to help us determine how to integrate the phosphor conversion LEDs and direct emission LEDs. The initial investigation of the optical modeling was to determine what wavelength is needed for the red direct emission LED to provide a warm white coordinated color temperature (CCT) of 2800K and a color rendering index (CRI) above 90. Various red LED wavelengths from 600 to 640 nm were explored. Figure 4 shows the results of the simulation. The various spectral power distributions of the warm white LED source module (wavelength and relative intensity of each component in the module - the blue LED direct emission, the phosphor converted LED emission and the red LED direct emission) are shown for various red wavelengths in Figure 4a. The effect of the red emission wavelength on CRI and efficacy of the warm white source module are shown in Figure 4b. A red emission LED with a wavelength between 615 and 625 nm can provide a CRI > 90. The shorter wavelength red LEDs require a lower relative power in the source module to obtain the 2800K color point. At wavelengths > 625nm both the radiation efficiency and the CRI are reduced due to the lower human eye response. Based on this modeling we targeted using a 620 nm red LED.

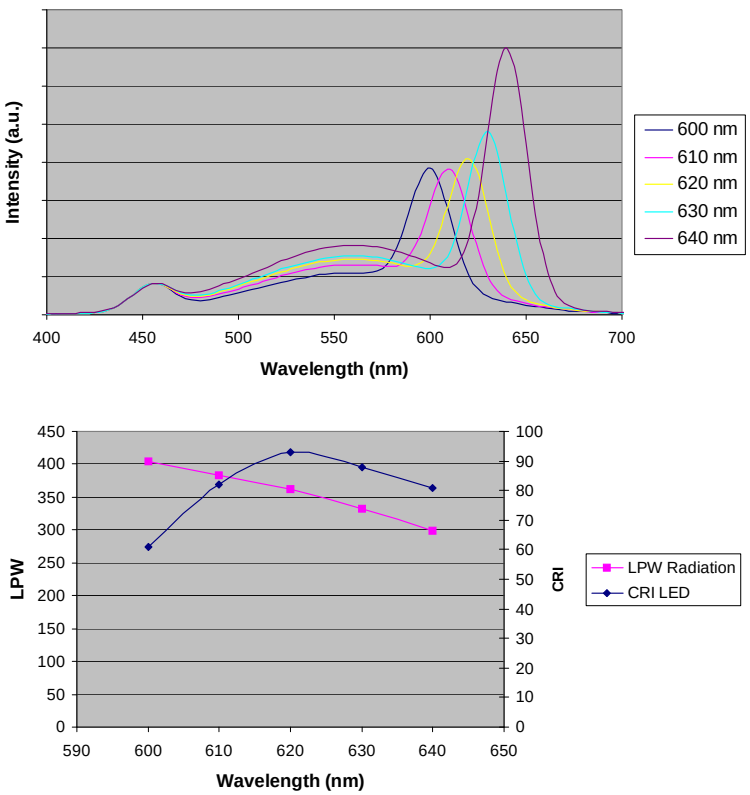

Figure 4: Optical modeling results showing (a) spectral power distribution of the warm white LED source module and (b) the effect of the red LED wavelength on radiation efficiency and CRI.

Integration of Direct Emission and Phosphor Conversion LEDs

For the warm white LED source module to have a small optical size with good color mixing, the phosphor conversion and direct emission LEDs need to be in close proximity to each other. A phosphor coating process was needed that is selective to the blue LEDs to allow their placement close to the red direct emission LEDs in the source module. Initial experiments were performed on a selective coating of the LEDs. The first step was to assess how the red LEDs are affected by the phosphor coating process. Red LED chips were placed in Cree's standard LED package and then a phosphor coating was applied to see the effect on the red emission. Figure 5 shows the results of this first experiment. The red chips were measured prior to phosphor coating and

encapsulation, after encapsulation (no phosphor coating) and after phosphor coating and encapsulation.

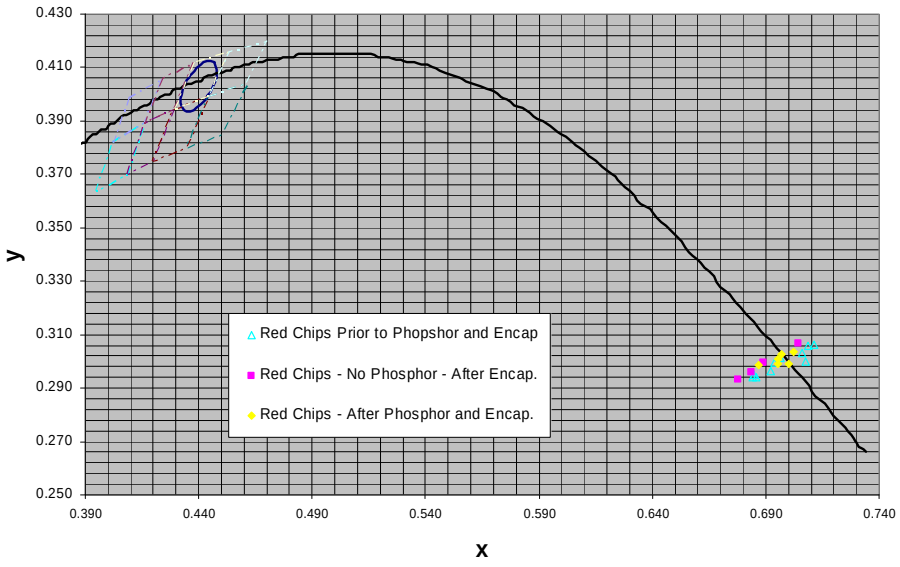

Figure 5: Color coordinated temperature x and y values for the red LED chips prior to phosphor coating and encapsulation, after encapsulation (no phosphor coating) and after phosphor coating and encapsulation. Cree's warm white LED bins are shown in the plot for reference.

Cree's warm white LED bins are also shown for reference. There was no color shift associated with the phosphor coating, showing that the selective coating concept is successful. However, there was a 13% decrease in the LED luminous flux after phosphor coat. The cause for this reduction in luminous flux is likely the phosphor and chip interaction leading to scattering losses.

We identified an optimum red LED wavelength from the modeling, and procured 620 nm red LEDs to build the warm white LED source modules. We also built proof-of-concept lamps to access the color uniformity.

LED Source Module

We continued working on fabricating a prototype of the LED source module. We designed application methods for the phosphor layer to selectively coat the blue emission LEDs but left the red direct emission LEDs uncoated. We then successfully developed a working process for the selective phosphor coating. This allowed us to characterize the white light emission from our source module for the first time.

We evaluated the correlated color temperature (CCT) of our first white source module to assess the chromaticity with respect to Cree's warm white LED bins. Cree's standard chromaticity regions are plotted on the 1931 CIE curve shown in Figure 6. The top figure shows the location of the Cree warm white bins with respect to the spectral locus (monochromatic light) and the black body locus. The lower figure shows a zoomed in view of Cree's bins. This project is targeting an LED source module with a 2800K color point, which are located in the Cree warm white bins.

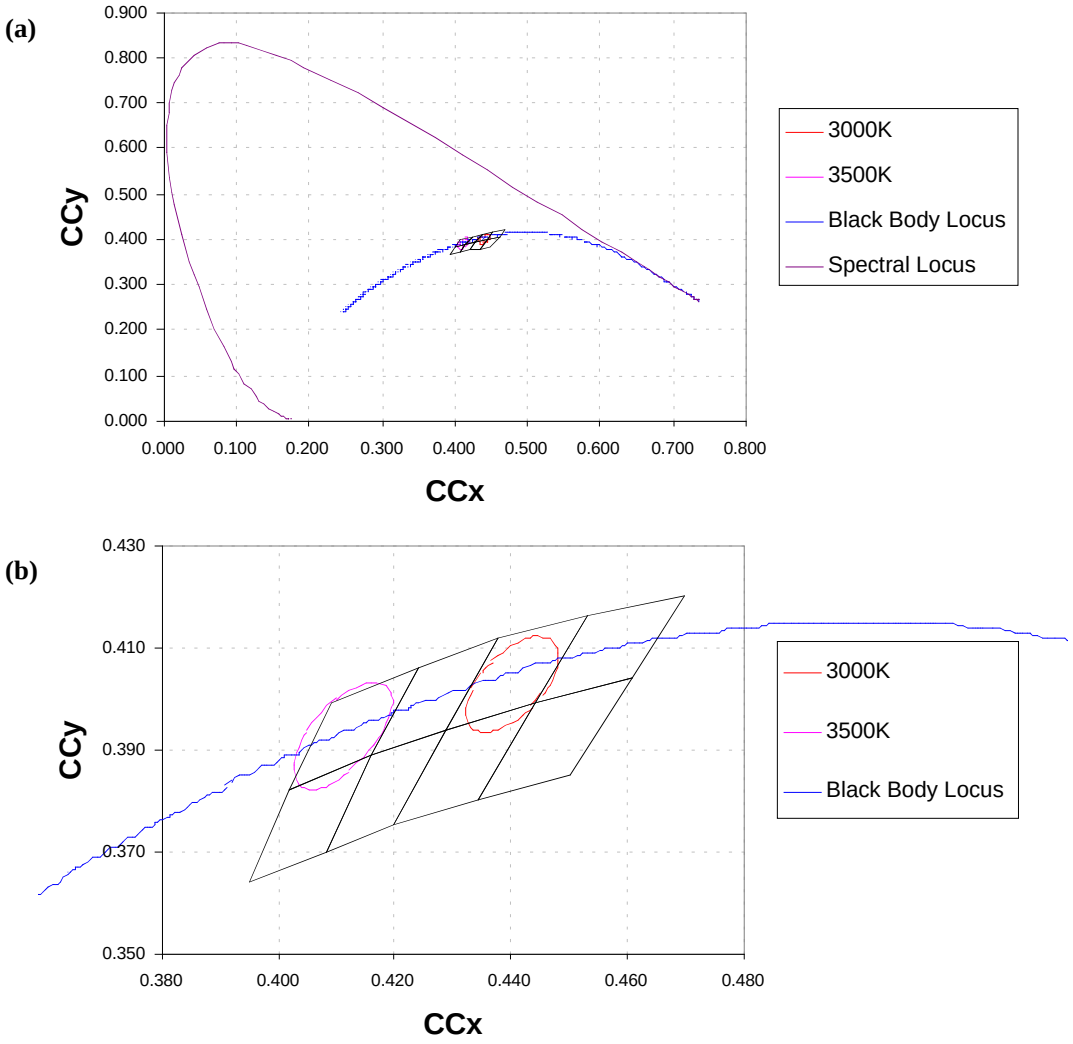

Figure 6. Cree's standard chromaticity regions for warm white LEDs (a) plotted on the 1931 CIE curve and (b) zoomed in on the warm white LED bins. Each black box represents one bin.

For the white LED source module, the resulting CCT depends upon the amount of phosphor material that is applied to the blue emission LEDs, as well as the amount of light coming from the red direct emission LEDs. To achieve the desired color point, both parameters need to be controlled together. We first varied the amount of phosphor material to achieve the desired CCT value of the Cree warm white bins while keeping the ratio of red emission from the direct emission LED constant. Figure 7 shows the results of varying phosphor material with the Cree warm white bins shown as reference. The spread of CCT is quite large from varying the amount of phosphor material applied but this range is far from the black body curve. We needed to fine-

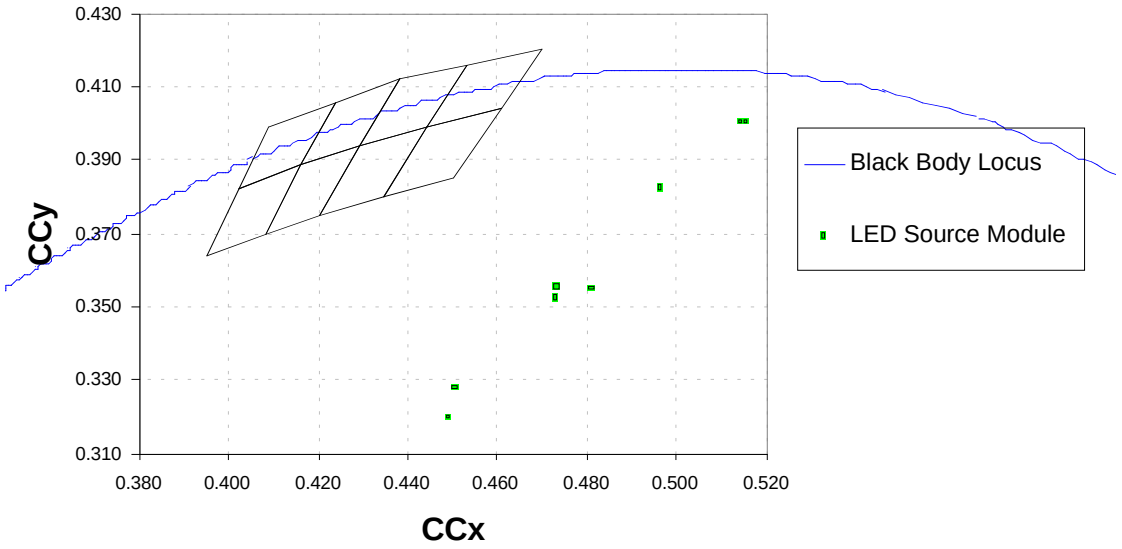

Figure 7. CCT values for white LED source modules with varying amount of white converter material on the blue LEDs. The Cree warm white LED bins are shown as reference.

tune our process to get the values closer to the black body curve. The easiest way to adjust this is to vary the amount of red emission from the source module by biasing the phosphor conversion and direct conversion LEDs independently. This required modification in the wiring of our source module. We later set up our testing units to allow for this independent control.

We also measured the spectrum of the LED source module and compared it to our optical modeling on the ratio of direct emission and phosphor conversion LEDs shown previously. The experimental result is in close agreement with the modeling, thus further supporting the model as an accurate tool.

We then optimized the performance of our first generation 26-LED source module prototype. Previously, as described above, we evaluated the color point of the source module to assess the chromaticity with respect to Cree's warm white LED bins. At the time, a few different current levels for the red and blue LED channels were investigated to provide the desired color point. We then performed a more detailed and systematic optimization of the LED module.

The detailed optimization work was performed by systematically varying the current levels of the blue and red channels. This allows us to characterize the optimum luminous flux and efficacy of the source module. Figure 8 shows the resulting color point of an array prototype optimized for a 2800K CCT with a luminous flux of at least 500 lumens. The blue and red channel currents were adjusted to maintain the desired color point and the luminous flux and efficacy of the array was evaluated at these different current values. The color point for three different red drive currents is shown as a function of changing blue drive current. Fine-tuning the current levels together allows the achievement of the desired color point closed to the black body curve.

The array efficacy is highest at the lowest red and blue current values due to the fact that each chip type operates more efficiently at lower current levels. On the other hand the luminous flux is highest at the highest drive current for the two channels. For the arrays, the efficacy was

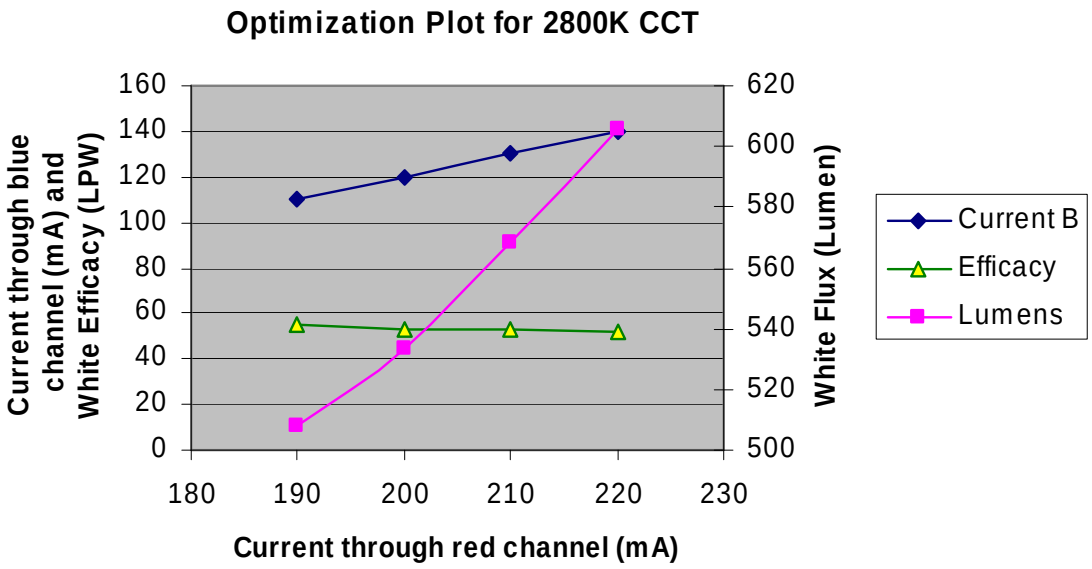

Figure 8: Optimization plot for white LED source modules with varying bias of the phosphor conversion (blue) and direct emission (red) LEDs. The luminous flux and efficacy was plotted for the various combinations of blue and red current levels needed to achieve a 2800K CCT.

maximized to 55 LPW with a flux of 508 lumens. At the highest current levels tested, the luminous flux was 606 lumens but with an efficacy of 52 LPW. A second array prototype showed an efficacy of 59 LPW with a flux of 527 lumens at the lower currents and an efficacy of 57 LPW and 617 lumens at the highest currents tested. Note that the data shown is for quasi-steady state measurements, which are not in thermal equilibrium but are held at bias for approximately 45 seconds (not instant-on). A 4% reduction in flux moving to a steady state measurement (5 minutes operation) was expected.

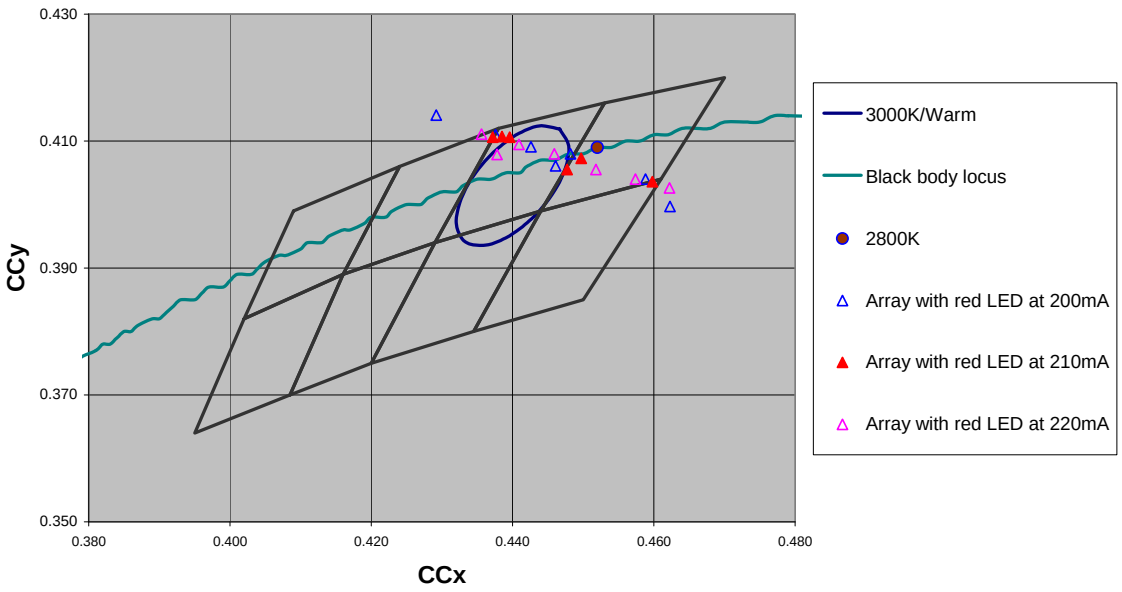

Figure 9: Color point values for white LED source modules with varying bias of the phosphor conversion (blue) and direct emission (red) LEDs. Three sets of data points are plotted at three different red current values of 200, 210 and 220 mA. The blue current level was varied to adjust the color point of the array to the 2800K target.

The detailed optimization with the first set of array prototypes was an important step in finding the operating conditions to maximize both luminous flux and efficacy at the appropriate color point. As usual, there is a tradeoff between efficacy and flux. The current levels were later selected to provide the best operating characteristics of the luminaire. We then completed building prototypes of a second-generation array using brighter LED chips to improve the flux and efficacy performance of the array. The arrays were optimized in a similar fashion to this first generation array.

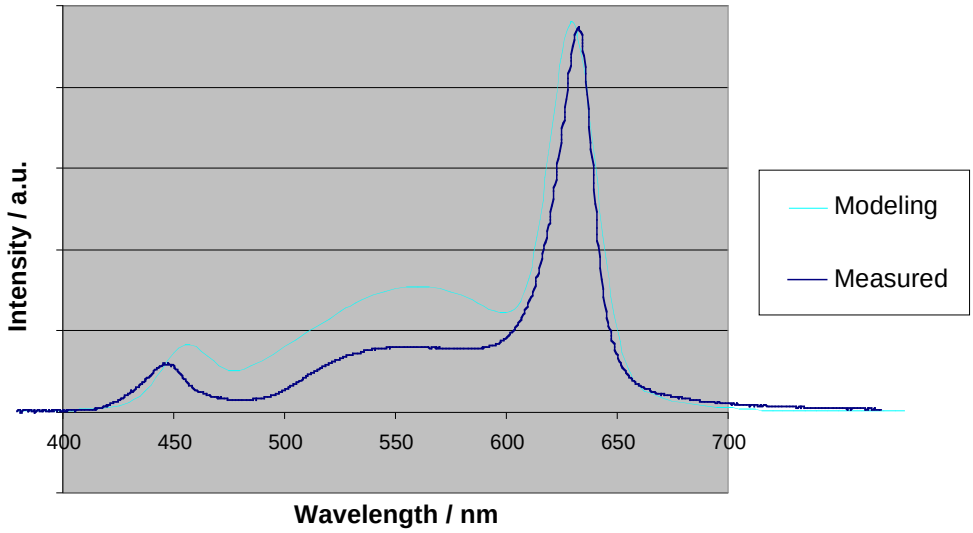

Figure 10: Optical modeling results showing modeled and measured spectral power distribution of the warm white LED source module. Note the blue pump and the red peak. Visually, this far more closely approximates an incandescent source than just white LEDs.

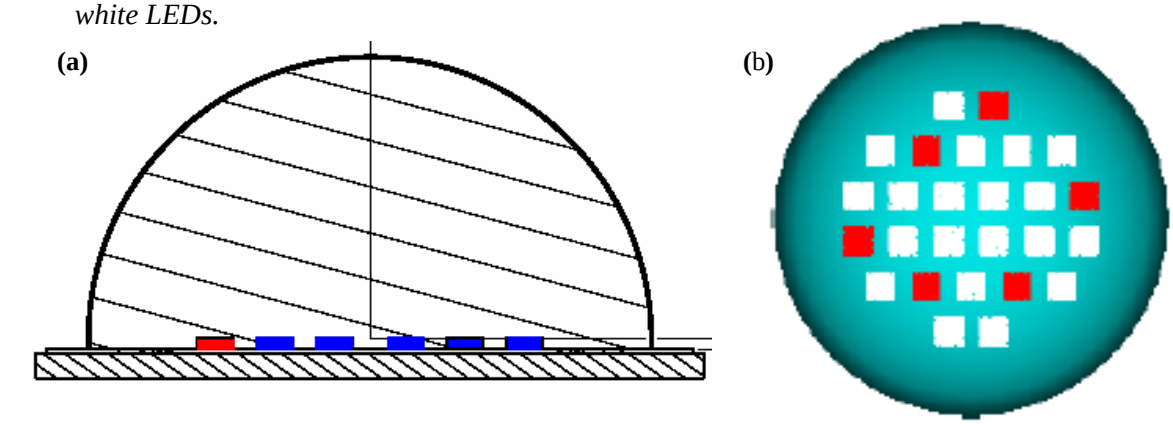

Figure 11: LED layout configuration for white source module shown in (a) cross-sectional view and (b) top view. Red squares represent the red direct emission LEDs and the white squares represent the phosphor conversion LEDs.

Optical Performance

We then investigated various layout designs using a ray-tracing based optical modeling program to assist us in picking the proper layout of the LEDs on the module. Two main configurations were investigated.

The near field and far field distribution pattern for each configuration, including CCT, were simulated. Good color mixing and uniform visual appearance are important when distributing the two different types of LEDs in the source module. In configuration A, the red LEDs are primarily located towards the center of the source module and in configuration B they are towards the perimeter. The geometrical pattern for the LEDs varies as well. In configuration A the chips are laid out in a hexagonal pattern, whereas configuration B is a simple cubic array.

The effect of the pattern geometry and the location of the red chips within the pattern could be seen in the simulations. Configuration A shows a far field pattern and CCT distribution that is

more reddish in the center than the edge. On the other hand, configuration B shows a more uniform far field pattern that configuration A. Though configuration B is better in terms of uniform CCT distribution, it still has some reddish warmer areas on the sides of the lamp. In both cases, the average CCT are higher than that of project target (~2800^{o}K).
The optical modeling was a useful tool to determine the best source module layout. Later, we continued to optimize the pattern of the LEDs and the placement of the direct-emission LEDs to yield a uniform color temperature and visual appearance at CCT of ~2800^{o}K

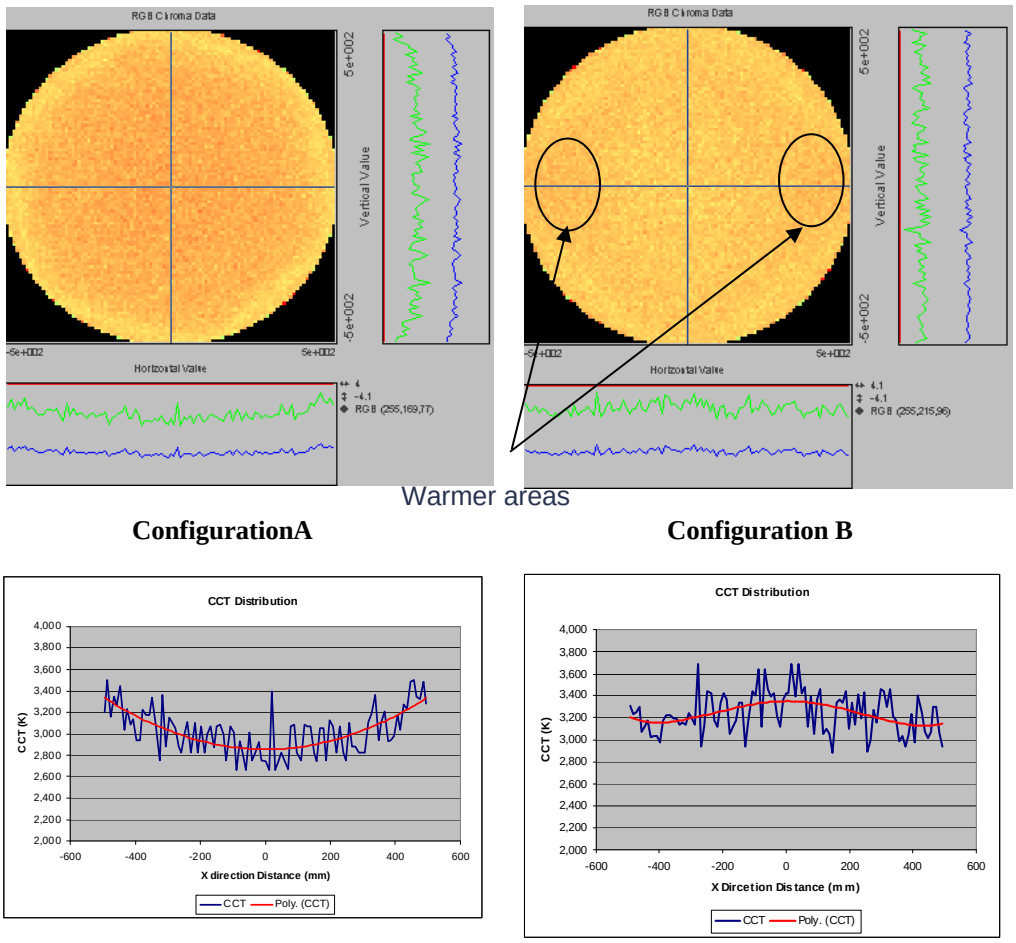

Figure 12: Optical modeling results showing the far field pattern and CCT distribution for the two LED source module configurations (A and B).

LED Module Design
Within six months of these studies we resolved a number of issues around specifying the design of the LED module in preparation for the development of full prototypes.

Die number: The number of die to optimize driver efficiencies and luminous efficacy is 25. Total calculated device count by Cree is 25 die, which includes both red and blue chips.

Die Ratio: The die mix is 19 blue and 6 red.

Die Size: Although CK had identified 400-micron dies as a sweet spot for cost, Cree has

suggested 700 micron chips, due to availability. They will be running at the lower currents and will be more efficient. The tradeoff in die size is then between cost (favoring smaller die) and efficiency (favoring running larger die at lower current).

Size: The enclosing circle for 25 of the 700-micron die is 7.2 mm diameter. Going to 600 micron does not gain much in terms of size (6.6mm). The overall diameter of the 25-chip system differs by only 0.6mm between 600 micron die and the 700 micron die. This approach also provides more leeway with allowable current density.

Light output: Desired light output is 800 lumens with a 5% margin. However, 800 lumens at 25C (steady state) was doable but there is an issue with output and a concern that the junction temperature could go to 90C.

Voltage: The nominal forward voltage for the blue die is 3.15V giving 59.85V across the entire string. Red Vf is 2.2 V giving 13.2V across them. No change or update in this specification. We were comfortable with providing additional power for the reds from the primary circuit without compromising overall power usage and efficacy.

Current: The current was approximately 0.142A for the blue die and 0.125A for the red die.

Power and efficacy: Power was calculated to be:

Blue – 19 die x 3.15Vf x 0.142A = 8.5W
Red: - 6 die x 2.2Vf x 0.125A = 1.65W
Total = **10.15W**.
Luminous efficacy is 800 lumens/10.15W = **79 lpw**.

Color Temperature: We targeted 2800K, and were able to tune up to 3000K but no higher than that for the applications we are targeting. Consistency in achieving this Color Temperature is important. Past research by others shows a consistent value of 5.5 MK^{-1} across the black body curve from 1800 to 11000K for perceptible differences. The importance is that perceivable variation at lower (warmer) color temperatures is much less, about +/- 50K. This simply means that variance in Color Temperature needs to be carefully controlled.

Primary Optic: We selected a silicone lens to cover the array and phosphor to cover the entire array as well. An identified risk was manufacturing a silicone lens larger than 5mm. We had concerns about the reliability of a large lens of that size. Issues include mechanical robustness, stresses in the material and cohesive failures under temperature cycling. This could be further exacerbated by the even larger size proposed.

See the figure below for the form and dimensions of a molded lens. Note that the diameter, 11mm, is larger than the array diameter, 7.2mm. This design expands the hemisphere to avoid the TIR loss issue at steep angles. See Figure 13 for the ray trace example that illustrates this issue.

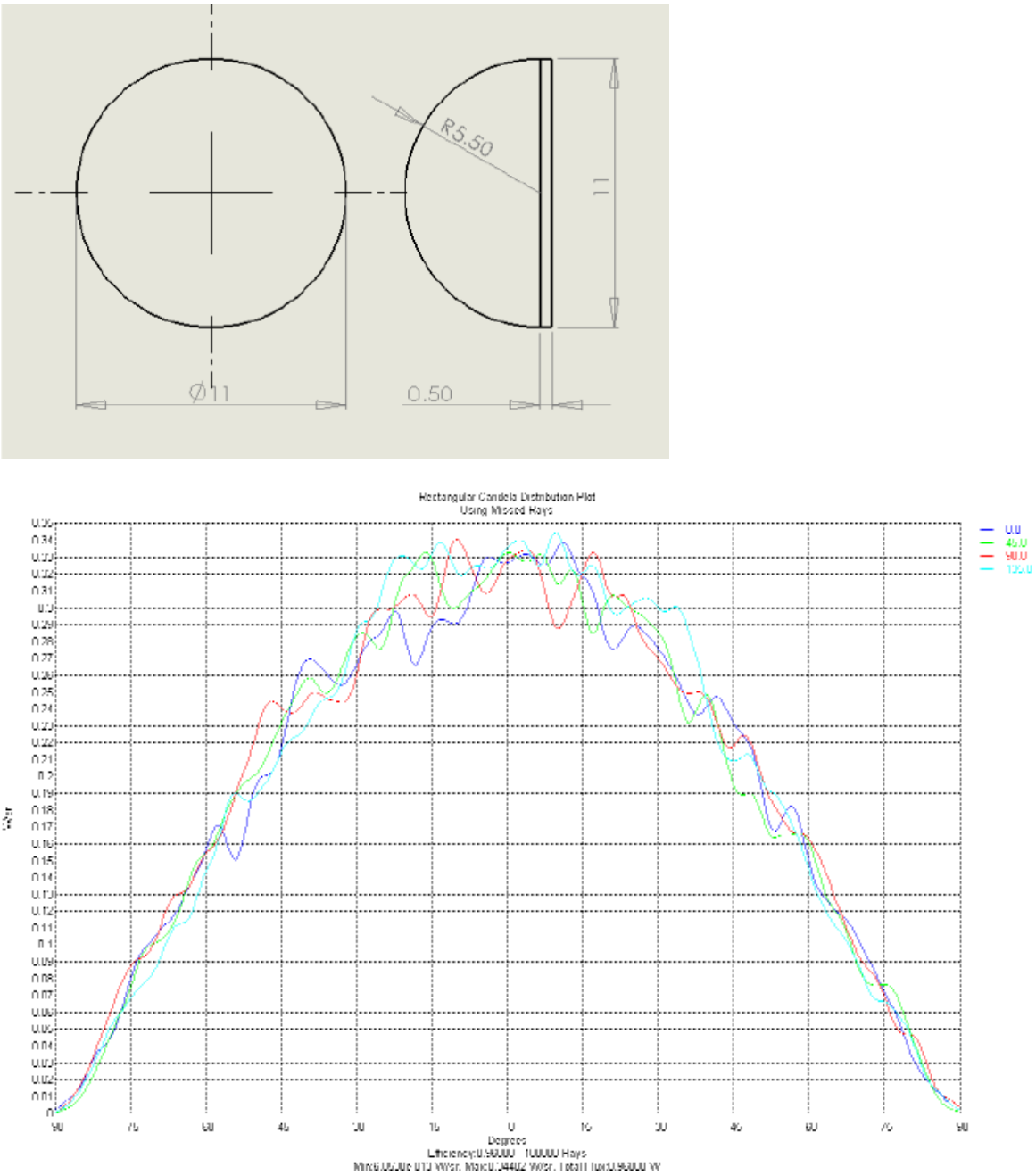

Figure 13: A rectangular candela distribution plot showing losses at various angles of light output as well as four slices across the top of the optic perpendicular to the plane of the array. This is the result of the trace of a single center die. For a side die the peak shifts but the drop off is similar.

In Figure 13, the distribution plot shows light distribution. About 4% of the light is lost due to Fresnel losses, which cannot be recovered. The key is that the diameter of the lens is substantially more than the aperture itself to reduce the high-angle losses associated with the walls of the optic. Additionally, the lens is not a perfect hemisphere and the center of the hemisphere is lifted to a point just above or coincident with the plane of the top of the die.

This diagram shows that the profile of the dome prevents light from being redirected towards the boards (lost) so that the secondary optics will be able to capture nearly all of the light coming out of the dome.

We then fabricated prototypes with 3-phosphor conversion LEDs and 1 direct emission LED. We evaluated the color point of the source module to assess the chromaticity with respect to Cree's warm white LED bins. We then varied the direct emission LED current to try and achieve the target CCT of 2800K. In addition, we varied the amount of phosphor material applied to the blue emission LED. Figure 14 shows the results of varying the current of the direct emission LED for two different amounts of phosphor material in LED Module D and E. LED module B and C data, reported in previous months, are shown as a reference along with the Cree warm white bins. As a reminder, LED module B contained one direct emission LED and varying phosphor material on the phosphor conversion LEDs. LED module C data was built with two direct emission LEDs and the current level was varied for these direct emission LED.

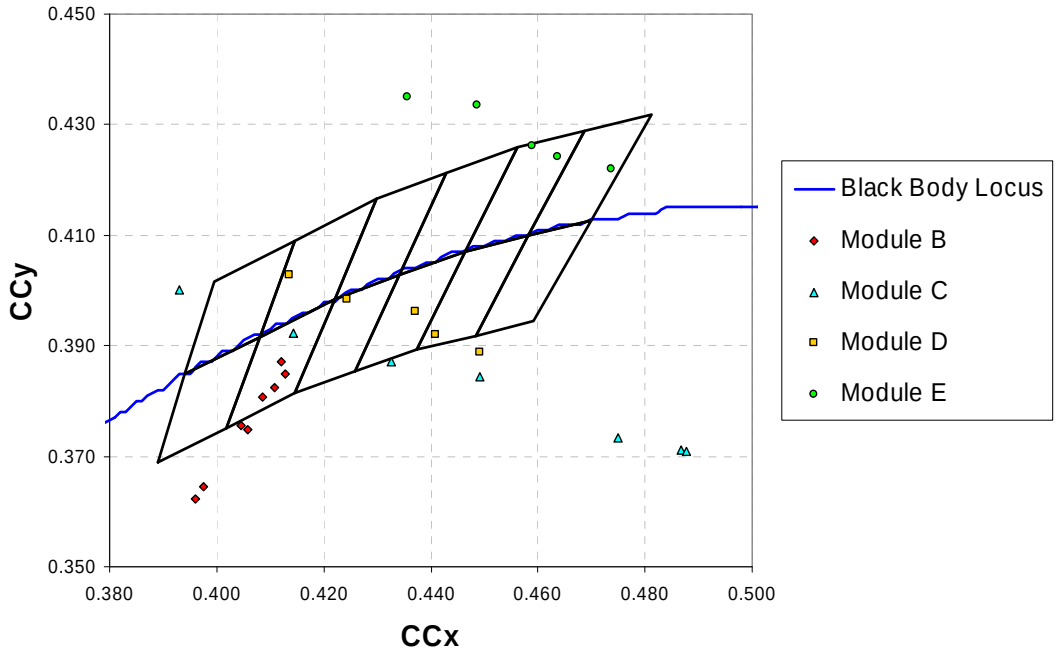

Figure 14: CCT values for white LED source modules with varying bias of the direct emission LEDs and varying amount of phosphor material (modules D and E). Variation in only the bias of the direct emission LEDs (module C) and variation in only the amount of phosphor material (module B), as well as the Cree warm white LED bins, are shown as reference.

The resulting color points of the white LEDs were found to vary along (more or less) orthogonal axes when plotted on the CIE diagram: the variation along one axis - along the diagonal from top left to bottom right - is due to the varying red LED flux with current bias in the white LED module; the variation along the other axis - along the diagonal from bottom left to top right - is due to varying amount of phosphor material in the phosphor-conversion LEDs.

For simplicity, we will refer to the red flux effect as the CCY variation and the phosphor amount effect as the CCX variation. Changing the current bias of the direct emission LED allows us to tune the color point in the CCX direction, as seen in Module C, D and E. Modifying the amount of phosphor material allows us to control the color point in the CCY direction, as seen in Module B. Comparing the color points for module D and E, which have a different amount of phosphor, you can also see this CCY variation. The offset between the two curves is due to the variation of phosphor material. Varying either the red flux or the amount of phosphor material can be used to control color point, but the red flux effect is the easier tuning mechanism to implement.

The amount of phosphor material between module D and E provides a large spread in CCY covering the majority of the warm white LED bins. These two modules will essentially provide the endpoints in determining the amount of phosphor needed. Tuning the direct emission LED current bias will provide the remaining degree of freedom to target the bins with the white LED modules. The CCT value of these two LED source modules varied between 2600K and 2900K, depending on the amount of phosphor material and red LED bias. These conditions gave us sufficient tunability to achieve our target CCT value of 2800K for the LED module. Additionally, these LED modules achieved CRI values between 87 and 89. These are very good values.

We then finalized our circuit layout design for the LED source module prototype shown above using the modeling data discussed previously to guide the design optimization. We then fabricated the prototypes of the current source module design with 26 LEDs.

We then designed and built third generation modules based upon the original design but ran into some problems with the red LED chips. The red LED chips characteristics changed from the beginning of the build to the end preventing us from taking advantage of the shorter wavelength die to improve minimize thermal effects on source module performance. We eliminated this degradation problem in later test builds and continued the generation 3 builds.

As a reminder, the generation 3 module would have lower red wavelength chips to compensate for the wavelength red shift that the red die see with increasing temperature in the source module at steady state operation in the luminaire. This lower red wavelength offers better CRI and higher efficacy range at operating conditions of the source module in the luminaire. Figure 15 shows these trends in the modeling work performed at the beginning of the project.

Source Module	Red Wavelength	CRI
Generation 2	625 nm	87
Generation 3	615 nm	91

Table 1: Summary of the effect of red LED wavelength on source module CRI.

The lower wavelength red chips did in fact have the desired improvement in CRI compared to the generation 2 source module. This wavelength shift of the red chips was able to improve the CRI from 87 to 91 between the Generation 2 and Generation 3 source module.

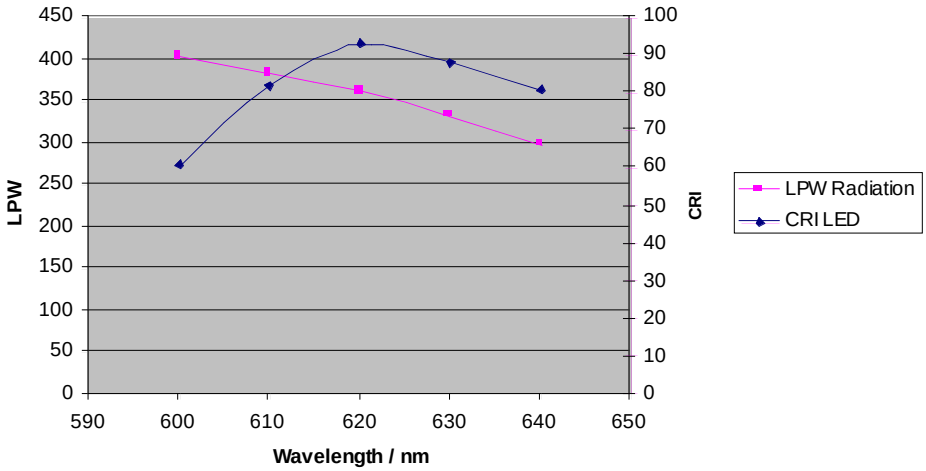

Figure 15. The effect of red wavelength on CRI and efficacy

We then explored building modules with new generation blue chips, requiring a new phosphor. A promising new phosphor application method was evaluated for the new blue chips to improve the luminous flux and efficacy. This new application method also had the potential in improving the yield of phosphor conversion LEDs for the source module. Changing the phosphor and application method though does require re-optimization of the color point to arrive at a module with the desired 2800K CCT at the black body curve. We then incorporated the new phosphor conversion LEDs in conjunction with the shorter wavelength red chips in the source module with good results. Additional developments continued in Generation 4 and Generation 5 modules.

High Temperature Testing

We initiated HTOL (high temperature operation lifetime) testing on 26 LED array lamp modules. The testing was carried out in an oven maintained at 85 deg C ambient temperature. We monitored the performance of the lamps undergoing the stress test at a week's interval over a month-long period. Both single-colored and two-colored lamps were subjected to HTOL testing.

A longer string containing 18 LEDs in series and the shorter string containing 10 LEDs in series are referred to as String 1 and String 2, respectively. The luminous flux, forward voltage (V_f) and the color coordinate *v'* were measured before and after the stress testing. The frequency of measurement was 1 week (168 hrs). In the figure below (a), (b), and (c) show respectively the luminous flux, V_f, and color coordinate *v'* variation with time for two single-color cool white lamp modules.

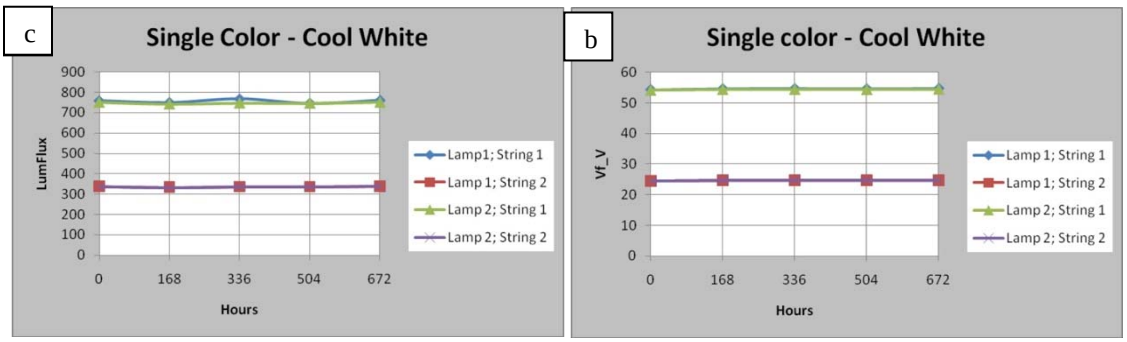

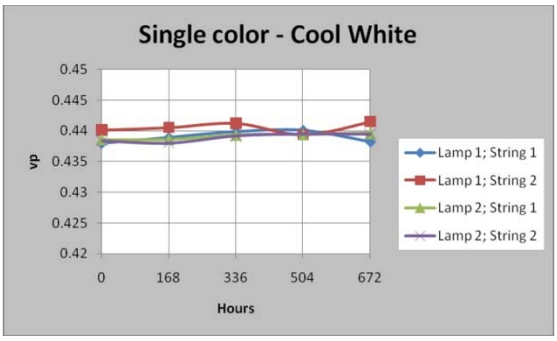

Figure 16: Variation of (a) luminous flux, (b) forward voltage, and (c) color coordinate v' as a function of time for two cool-white 26LED array modules.

From the figures, it is very clear that there were minimal changes in the key metrics after 672 hrs of HTOL stress testing. Similarly, two two-colored lamps were subjected to HTOL stress testing, and till date we have 168 hrs of reliability data. String 1 and String 2 refer to the string containing the yellow-green and red string, respectively. Figure 17 (a), (b), and (c) shows respectively the luminous flux, forward voltage (V_f), and correlated color temperature (CCT) variation with time for two two-color systems.

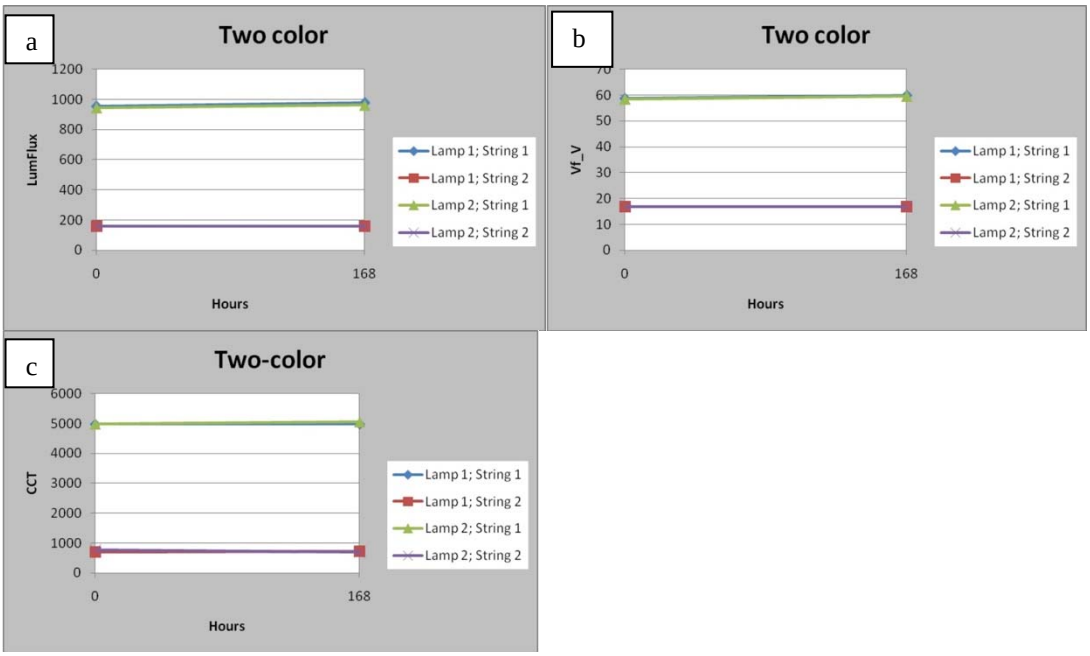

Figure 17: Variation of (a) luminous flux, (b) forward voltage, and (c) CCT as a function of time for two two-colored 26LED array modules under HTOL stress-testing.

Similar to the single-color modules, the two-color modules showed very minimal change in the key metrics after 168 hrs of HTOL stress testing.

In summary, we initiated 85 ^{0}C HTOL testing on both single-colored and two-colored parts fabricated using a production tool. Minimal variation was observed for the luminous flux, forward voltage, color point and reverse leakage current after 672 hrs of testing for the single-color parts and 168 hrs of testing for the two-color parts.

Electrical Driver Technology

We also directed a significant effort towards efficient power supply development with successful efficiency improvements in new configurations. The fundamental approach we took was to examine energy transfer arrangements and control methods. This design was *not* a complete power supply, but rather was intended to expose choices that affect efficiency.

This design was intended to be a single-stage high power-factor buck converter. This is based roughly on the high power factor fly-back design, which we used in one of Color Kinetics' line voltage products. The buck topology is really only useful for output voltages between about 1/5 to 1/3 of the peak line voltage, or about 34 - 60 volts output for a 120V line. In this design, output power was intended to be about 10 watts, for an average current in the 150mA range. This value was aligned with our desired power level for the DoE program.

Earlier attempts resulted in efficiencies in the 85 to 88 percent range. This is an efficiency range that is very good, but not exceptional, for good quality switching power supply configurations.

After a series of simulations, in a series of real experiments, we evaluated inductor values, modified switching frequencies, and component values. Altering the inductor design improved efficiency by about 3-5 percent. Reducing switching frequency by 50% to a maximum of 150KHz resulted in a 2-3% improvement. Switching induced noise appeared to have some oscillation issues that will be the focus of future work. Finally, adding capacitance to the input helped as well. In this design we used a standard ES1D silicon diode. Though this diode is quite fast, slowing down the transition rate of the switching field-effect transistor (FET) improved efficiency slightly.

As a result of this evaluation and improvements, early results were over 90% transfer efficiency. Power factor was good, but more analysis was required. We found that care must be paid to losses in startup and operating modes. As one example of this, the 5mA required to run the control chip represents 1% of efficiency! This is an important lesson – the solutions themselves may detract performance and increase cost. Startup circuits typically run about 1mA constantly. That is unfortunate because this also represents 1-2% at 120-170V peaks. We were deep in the details and squeezing out as much efficiency as we can without incurring high costs in the power stage.

We then continued the development of power supply configurations and evolution to provide more efficient solutions. Investigation began with a transformer design to provide the necessary power configuration. Testing revealed that we could indeed build transformers to provide all of the necessary voltages. We put together an over-sized transformer, which also contained a winding to allow the control chip to run on its own power. Results did not materially differ from the previous results, except that, as predicted, the efficiency was slightly less because of the additional power required to drive the control chip.

This was not an entirely satisfactory design, but it was intended to be a "no compromises" type design that can provide up to 30 watts of output power at high efficiencies. Later experiments were designed to determine the sources of loss in the high voltage buck converter design, which we also developed. One outstanding question was how the reverse recovery time of the output diode would impact efficiency. Though it is well known that reverse recovery time of silicon rectifiers at high voltage does affect efficiency, it is never easy to find out just how much.

The basis of the design depends on a variety of diodes. Luckily we could change diodes, and in

test systems, we could also adjust conditions such as diode temperature. Reverse recovery problem gets exponentially worse at high temperatures, high currents, high voltages, as well as at higher frequencies. We made some headway by decreasing the slew rate of the power transistor. We also used a silicon carbide Schottky diode in place of the ES1D silicon diode.

With this new configuration, efficiency increased by almost 1% at high power. Smaller effects were observed at lower power levels, and some efficiency loss was observed at very low levels, where the old diode was not helping much anyway. This effect is caused by the increased capacitance of the SiC diode, as well as its higher Vf.

That efficiency increased at high power is extremely important, since it indicated, that even with the additional 70pF capacitance added to the switching node, and the increase in Vf, the elimination of reverse recovery made an important difference.

We estimated that the output diode's Vf alone accounts for 2.1% loss. Another 1% is lost in switching capacitance. Given that the total loss is only 7.3%, it suggests that reverse recovery was a huge part of the total losses in the ES1D, and looking graphically, probably accounted for most of the drop in efficiency at higher power levels. These were good results and showed that improvements can be made to existing high efficiency configurations.

An interesting side note, we considered the use of Cree's GaN diodes. It would have probably gained another 0.3-0.5%, and we can confirm the usefulness of continued work on this as part of a DoE initiative. Interestingly, this is a Cree developed part developed under other government programs for many applications. These are more expensive than other high-speed diodes but the additional cost may be outweighed by total cost of ownership issues, less heat dissipation and higher reliability.

Efficiency stood above 92.5% at all voltages.

We continued development on the power supply and drivers side and completed some early prototypes. Features included:

- Near "Instant On" feature that also allows for power reduction on operating current
- 92% efficiency.
- Should be able to dynamically control each LED string in manufacturing.
- First generation prototypes based on our designs are shown below.

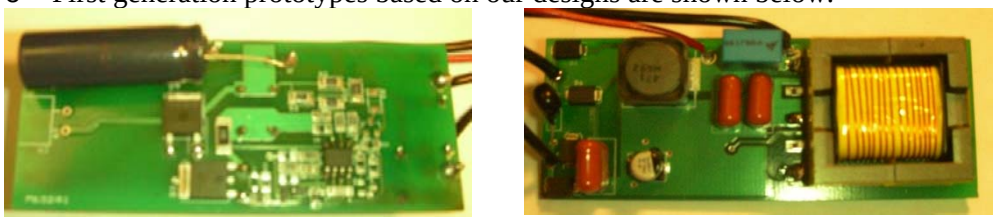

Figure 18. Power supply prototypes

Another challenge was the ability to package the driver electronics into the base of a replacement lamp form-factor. As a result, we analyzed the geometry of the power supply to fit it within the package.

Below is shown a geometry for the power supply configuration. As you can see from the images, the transformer and the capacitor are the two components that are the largest and the most

difficult to arrange in a fashion that allows the entire assembly to work.

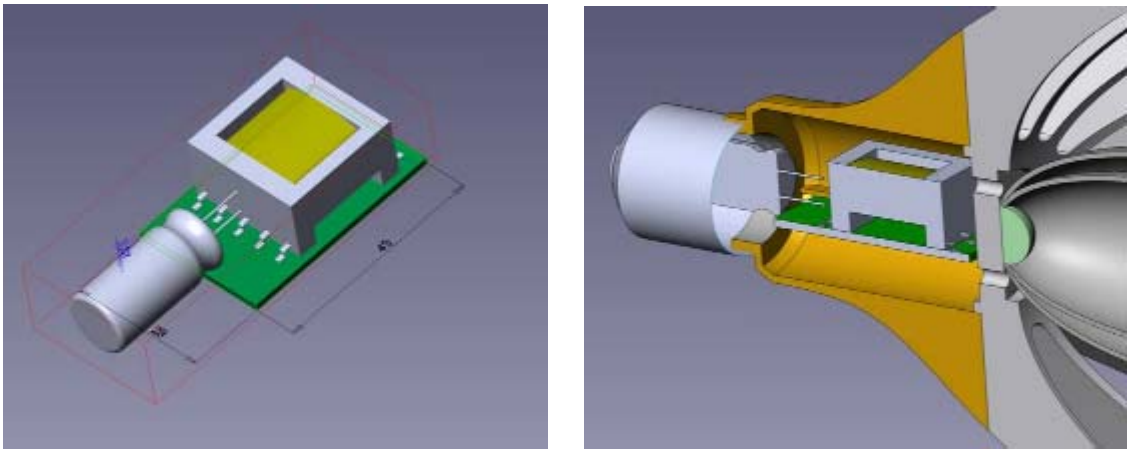

Figure 19. Power Supply Configuration

Thermal Modeling

We examined how a large module would integrate into a lighting system fixture. Integration is not simply the placement of LEDs on a metal housing and is not just one of mechanical, thermal, optical or electronics control.

The primary drive circuits depended largely on the series-parallel configuration of the LED die and while we did this in the past for traditional devices, this approach required a new interconnect for the luminaire/lamp. In order to make the program goals more accessible to the market we are strongly considering a non-traditional module approach rather than a specific luminaire design.

Integration of drive electronics will present issues for thermal and may require complete isolation of the drivers from the LED portion of the system, but this needs further study and depends, in large part, on the final LED module.

Thermal modeling and the feed-forward control are just at the beginning stages and we are in the process of developing this notion further.

Based on the developing mechanical design of the complete system, we modeled thermal management of the unit before committing to physical prototypes of the Par 38 modules. Some of the resultant analyses are shown below. The colors and lines correspond to temperature (blue – cool, red –hot) and airflow.

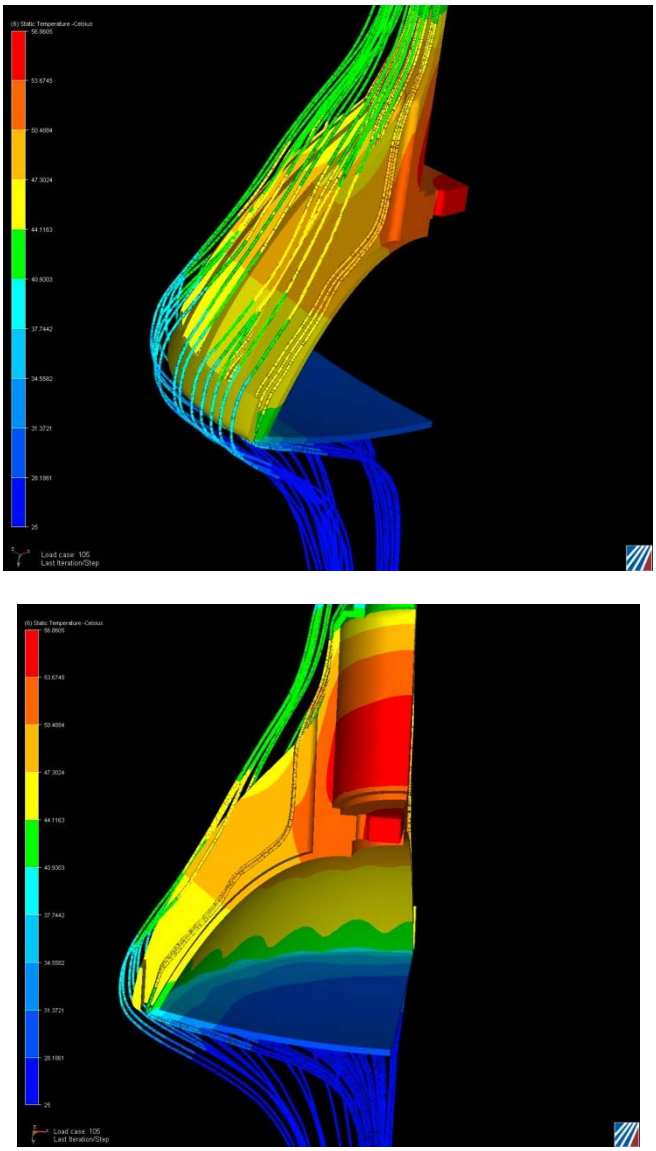

Figure 20. Thermal modeling simulates the air flow surrounding the lamp and the conduction of the materials to calculate the temperatures that the light engine will see.

The assumptions for the thermal analysis included a 10W heat source for the LED engine and tracking the heat flow out of the engine into the 'cage' of the lamp. At this point, based on the simulation, the heat sinking capability was sufficient for the power dissipation. The margin is close however and we did not know if this will hold true for a lamp product in all conditions.

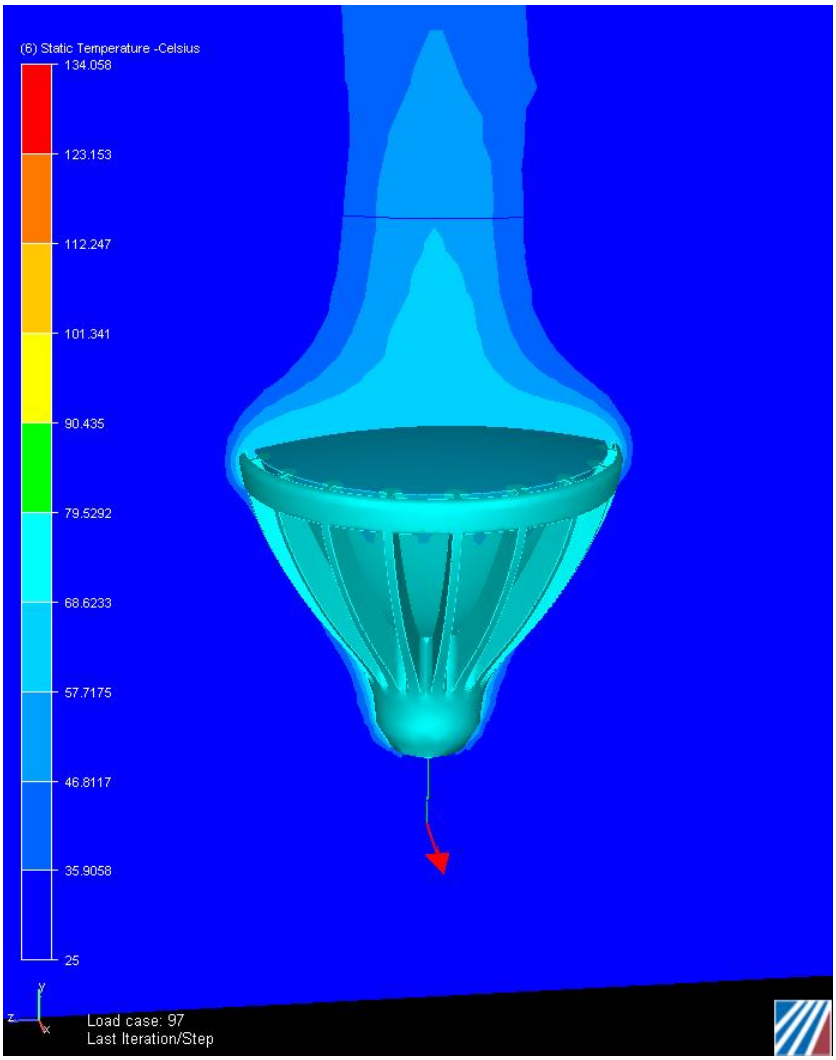

Figure 21. Several variations of thermal analysis has revealed that the dissipation mechanism appears to be good for several orientations. Final performance, of course, will be determined with the physical prototype.

We also built prototypes using 3D printers (not shown), to evaluate overall configuration and appearance. This has also assisted in packaging aspects for the power supply, which will fit in the base.

LED Engine Testing

The LED engine was attached to a heat sink and connected to the first full version of the power supply circuit.

Figure 22. A milestone: Brad Kolsky and Ihor Lys demonstrate first light from the LED Engine and power supply.

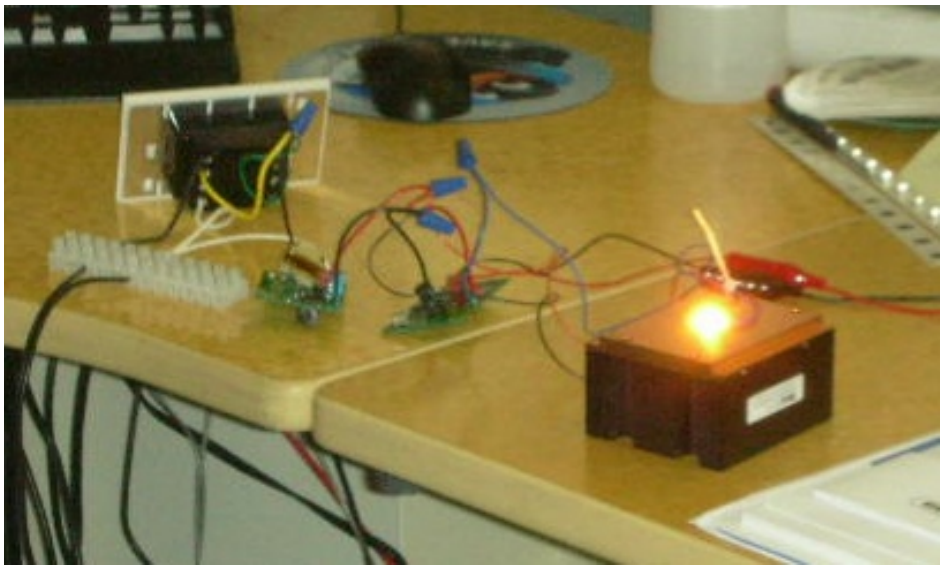

Figure 23. Closeup of the LED engine on heat sink and power supply on the bench.

As shown in figures above, a thermocouple was attached to the edge of the ceramic substrate and the ceramic assembly was soldered to the pads on the metal core boards. The heat sink is a copper covered graphite heat-sink and is for test purposes only.

Figure 24. Test configuration for the LED engine performance test. The LED package was mounted to a metal-core board from another prototype fixture and tested in situ for light output.

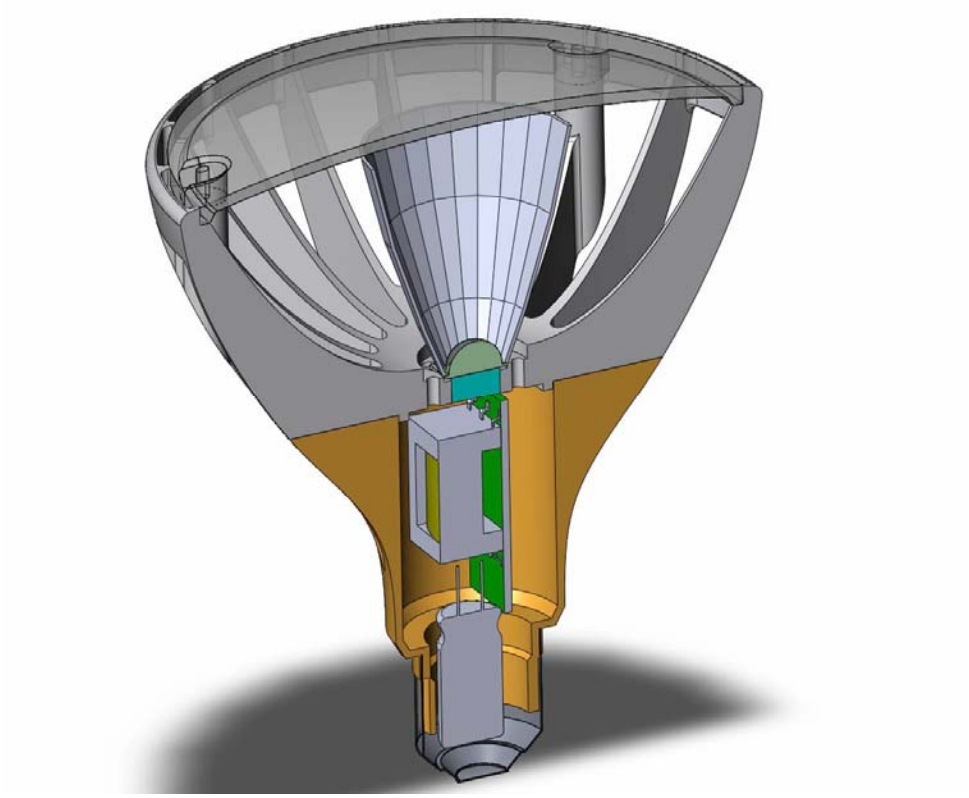

Figure 25. The complete CAD design of the PAR38 LED lamp system was also completed during this period.

The mechanics and optics portion of the system were completed and fabricated. The power supply system, shown in the base section of the figure above, was an earlier design.

Figure 26. These images show the mechanical prototypes of the 'cage' heat sink and base unit.

Mechanical Prototyping. In addition to completing the design, we prototyped the mechanical parts of the PAR 38 module. The cage, as shown in the left hand side of Figure 26, incorporates a copper slug and features for press-fit of the secondary optic. Holes in the base of the cage allow for conductor pass-thru and fins provide substantial surface area for heat dissipation.

Optical simulation. One important aspect, for the final product is the resultant far field distributions of the blue and red channels of the LED engine and the complete optical system. Using a 90% reflective surface the optical system efficiency is ~83% and the beam angle is ~25 degrees FWHM.

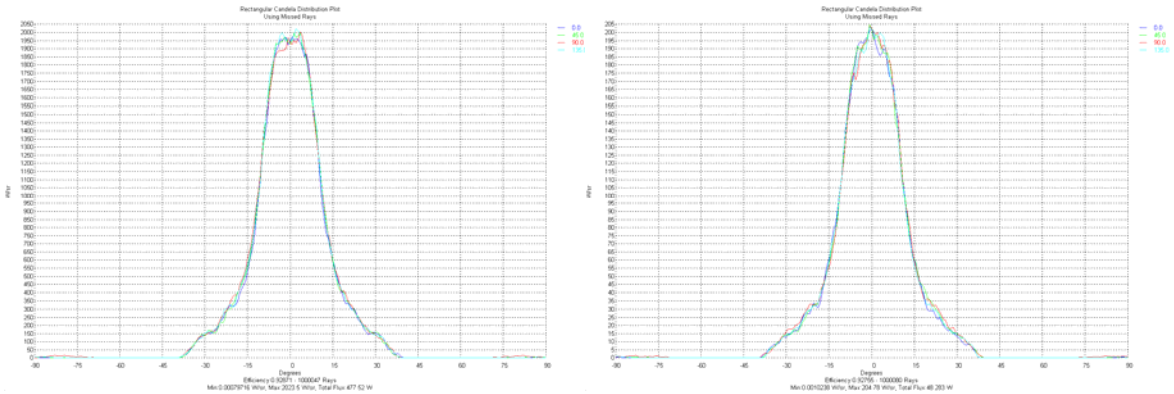

Figure 27. The angular distribution of the lighting output of the blue (left) and red (right) channels respectively. The issue is to insure they are as close to identical as possible.

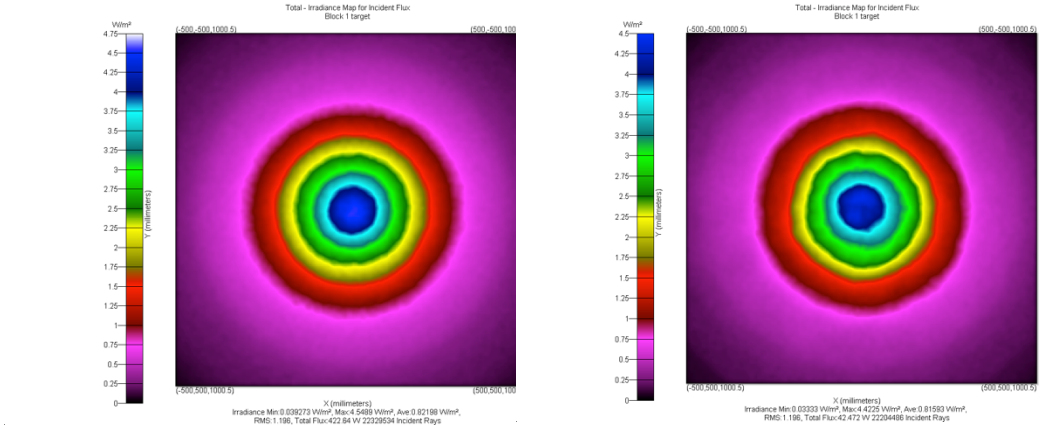

Figure 28. Irradiance Maps of the Blue and Red Channels

Irradiance Maps of the Blue and Red Channels. Color uniformity is extremely important. The maps of the figure above are false colored for the purposes of interpretation. By subtracting one graph from the other we can approximate the color uniformity of the final output. If variation is less than 5% variation it will not be visible. Variation of between 5%-10% variation *may* be visible and variation of greater than 10% *will* be visible.

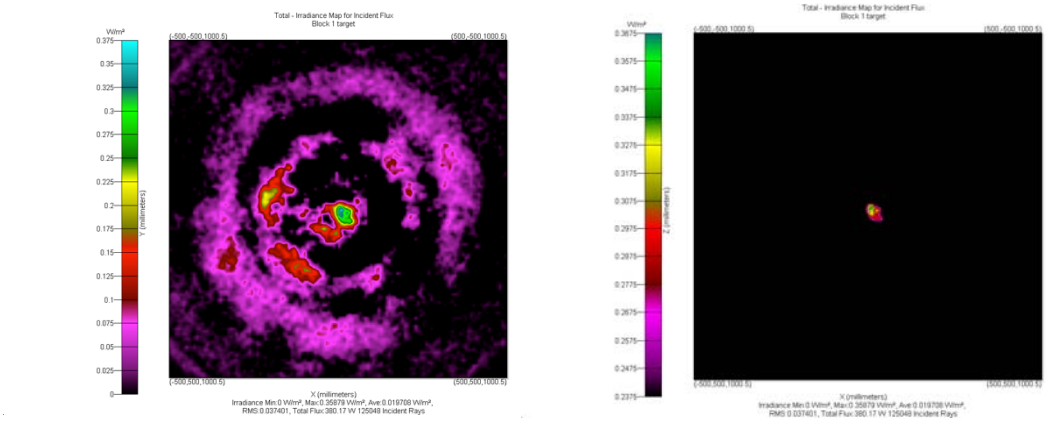

Figure 29. The difference map, shown on the left shows regions where differences are mapped to false colors. The right hand image is the map of where the color differences are greater than 5%.

The simulated results were quite promising. The overall color uniformity is quite good though a few small sections of the spot may not appear uniform. (5%-10% range) There are no non-uniformities greater than 10%. The non-uniformities cover a small angle (less than 1 degree), so a 5 degree holographic diffuser will be able to clean up the pattern sufficiently if there are any issues. Thus, our plan was to augment the secondary optic with a low loss holographic diffuser to further homogenize the output.

As with any simulation however, we have concerns and warn that optic performance may not meet the simulation because:

- The rayset data was from only one select source.
- The silicone dome geometry and/or texture may vary from measured data.
- The molded part may differ from the CAD.
- The coating reflectivity and/or specularity may differ from simulation.

LED Source Module

We completed an initial design of the LED source module. In order that the warm white LED source module have a small optical size with good color mixing, the phosphor conversion and direct emission LEDs needed to be in close proximity to each other. We designed our circuit layout to allow for this close placement of the direct emission and phosphor conversion LEDs, as seen in Figure 30. The LED source module initially contained 4 LED chips in a closely packed arrangement to achieve small optical size and color mixing. With the red and blue direct emission LED, we designed

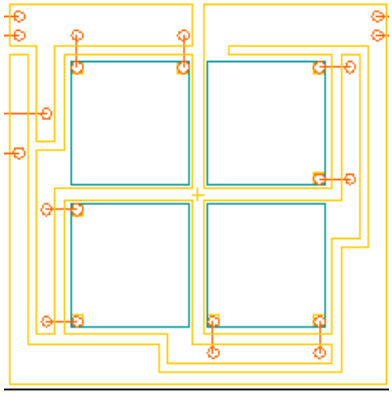

Figure 30: Schematic of LED source module circuit layout.

application methods for the phosphor layer that are required for generating warm white light. This was a significant technical challenge to yield a combination of the emitted blue and red LED light sources. However, the result was worthwhile; the down-converted light generated by the phosphor layer results in a warm white light having coordinated color temperature (CCT) of 2800K and a color rendering index (CRI) above 90 which were right on target.

Based on our initial design of the LED source module, we proceeded with our procurement for the substrates and components required for this design. As shown in Figure 31, we used a LED test module for evaluation this month. In these initial parts we have worked on the material selection in close proximity to the LED chips. We have also been working on attachment and assembly procedures for the LED chips. The height difference of the direct emission LED and the phosphor conversion LED also needs to be considered in the assembly procedures.

Design

As the various dimensions of the substrate, primary lens and power supply came together we worked on the detailed iterative tasks of configuring the lamp/fixture system to incorporate all of these developments. Regarding the secondary optic, one thing was clear – no pun intended – the optic required for a relatively narrow angle of 25 degrees will be much larger than a wider angle optic. The size of the optic is a function of angle and the smaller the angle, the larger the optic. We pushed for the narrow angle because the market opportunity for spot projection offered the most market opportunity. However, we focused on squeezing all of the components into the Par 38 form factor and we did succeed at accomplishing this.

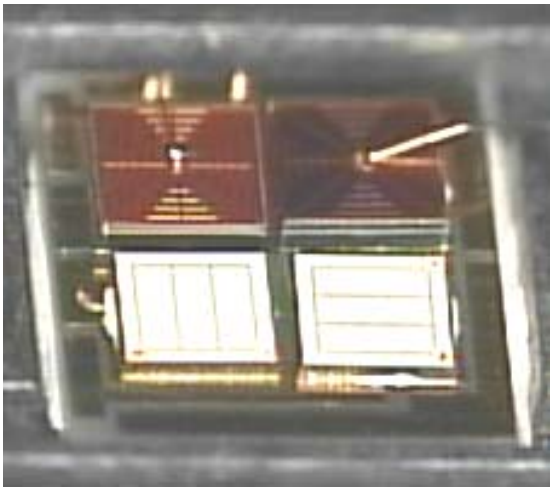

Figure 31: LED module prototype with 2 direct emission LEDs and 2 phosphor conversion LEDs.

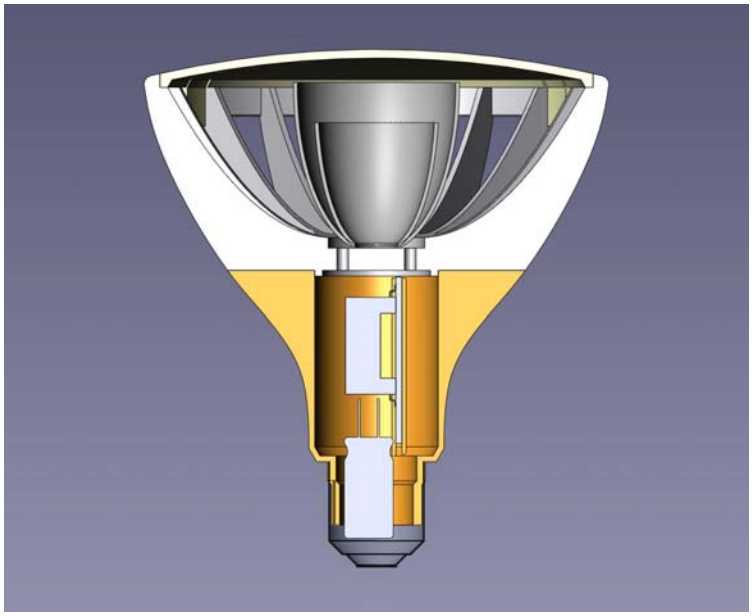

Figure 32. The overall form factor of the current design is that of a PAR 38 lamp. We managed to shoehorn all of the elements into this geometry including the power supply, optics, and LED engine.

We continued to refine the design over many months, integrating and assembling and testing units and subsystems on a frequent basis. The final design is shown below.

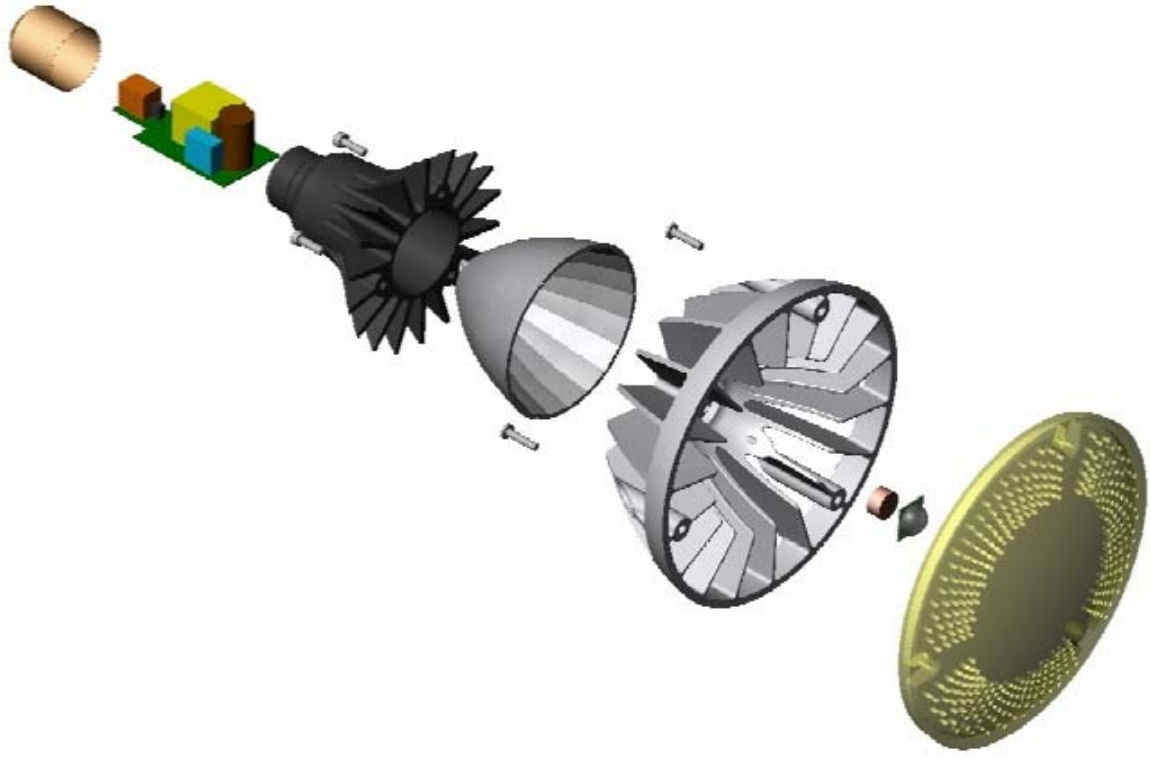

Figure 33. The PAR38 current design with the perforated cover and complete assembly.

LED Controls

We made significant efforts in a control system to provide warm-up compensation of the lamp output in color temperature. Our original approach was a feed-forward approach to model the system and then compensate using the developed model but we then developed a feedback model using a small thermistor to actively measure temperature.

Although AlInGaP materials used in red LEDs will increase in wavelength as the temperature of the LED die increases there are compounding effects of temperature on the drive electronics as well. The resultant white light in the hybrid approach will also shift perceptibly. This characteristic is undesirable in any commercial product and we have focused efforts in the control of the two strings to compensate for this temperature effect.

By actively adjusting the output of the blue LEDs during this warm-up time, the overall light output can be fixed to a particular value of color temperature. More precisely, we are controlling the ratio of red to blue current since we cannot control the currents individually by fixing the red current and changing the blue current. This is done by actively compensating the overall current as the unit operates.

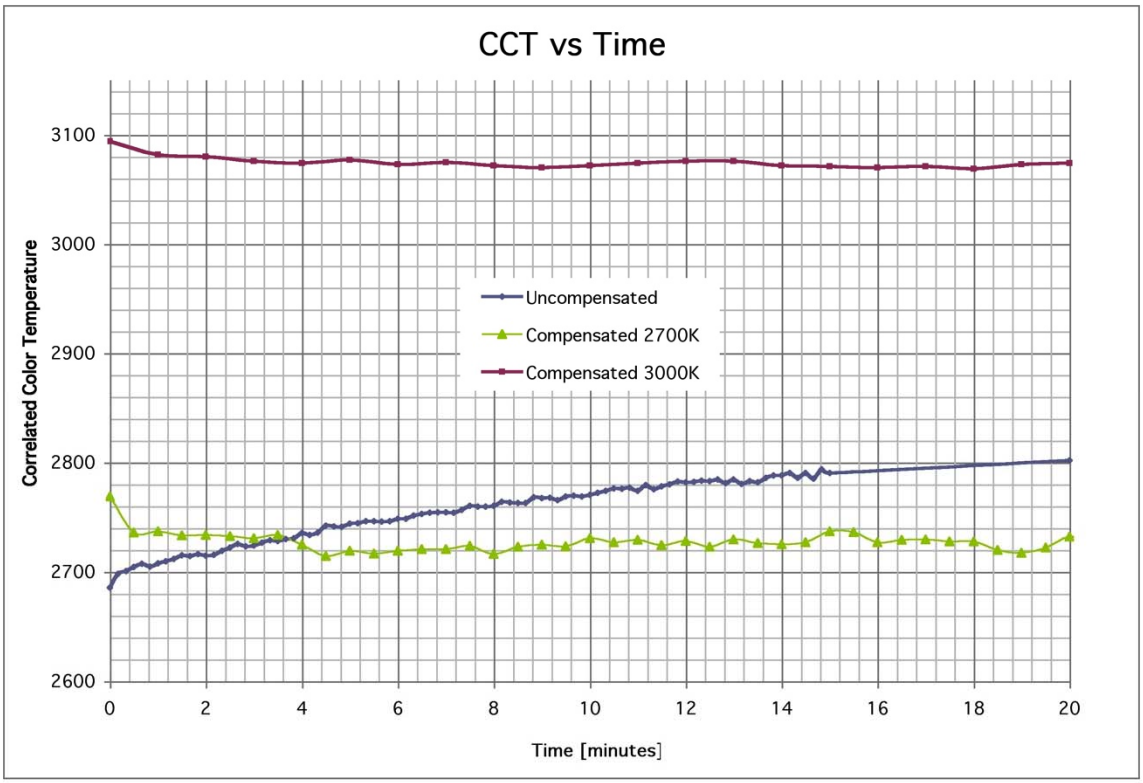

Figure 34: The uncompensated lamp varies significantly in color temperature output over a 20 minute period. With the compensation circuit not only is the color temperature variation reduced to an imperceptible level but the color temperature value itself can be set to different levels. The green and red lines show 2700K and 3080K flat line outputs respectively.

As shown in Figure 34, the results are very promising and show that this modeling and feedback system is very effective at eliminating the color temperature shift and providing a specific color temperature value. In the uncompensated data, the shift of over 100K would be noticeable at color temperatures in the 2700 to 2800K range. This would not be an issue for high color temperatures – for example at 5000K or above since 100K shifts would be imperceptible.

Generation 5

In the last version, Generation 5, module we attempted to improve CRI and light output by adjusting the ratio of blue and red LEDs. By reducing the number of red die and increasing the blue die by four, we hoped to balance the currents and improve the output of the system. Unfortunately, to make a long story short, these changes did not improve the system performance. Lumen output improved only slightly but the overall efficacy went down. See Table 2 for a detailed comparison. We went back to the previous ratio of red and blue die.

Metric	Generation 4	Generation 5
Luminous Flux (lumens)	681	723
CRI	91	93.2
CCT	2716K	2724K
Power Factor	0.9	0.9
Efficacy (lpw)	69	60.5
Beam angle (deg)	25	25

Table 2. The key difference between Gen4 and Gen5 was a significant 15% drop in overall efficacy. The other metrics were good, but the loss in efficacy means that the Gen 5 approach will not be pursued.

Conclusions

While challenging, we were able to achieve a record performance during the course of the program for a complete LED lighting system that met or exceeded our goals for a replacement lamp form-factor, a PAR 38, that is both technically advanced and practical enough to target market opportunities in LED lighting. A remarkable team comprised of LED experts and systems experts was able to conceive, design, test, and build a lamp of great performance. We learned much from this program and continue to apply the lessons learned to new LED and electronic systems.